

resonance measurements. In this case, the thin-sample reflectivity as a function of field was measured also. The results are quite striking, showing changes in reflectivity in qualitative agreement with the fact that the changing index of refraction causes the fringes to shift.

#### ACKNOWLEDGMENTS

We wish to thank Dr. R. Braunstein and Dr. L. R. Weisberg of RCA Laboratories, Dr. W. Beyen of Texas Instruments, and Dr. F. A. Cunnell of Services Electronics Research Laboratory for supplying samples. We are grateful to Professor H. Yoshinaga and Dr. A. Mitsuishi of Osaka University for giving us new data

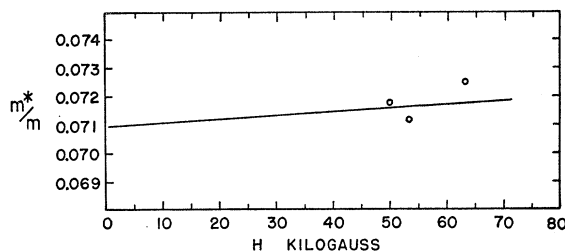


FIG. 2. Cyclotron resonance effective mass ratio vs magnetic field for GaAs at liquid nitrogen temperature.

on the reflectivity of the reststrahlen bands of CsBr, CsI, and KRS-5. We also thank A. Mister, R. Anonsen, and W. Cline for operating the Bitter magnet.

## Exciton-Induced *F*-Center Growth in KI and KBr Crystals

JAMES H. PARKER, JR.

*Westinghouse Research Laboratories, Pittsburgh, Pennsylvania*

(Received May 31, 1961)

A study has been made at room temperature of the growth in *F*-center concentration resulting from the absorption of photons in the energy range of the first fundamental band (exciton band) of KI and KBr crystals. The growth in *F*-center concentration was followed by measuring the fractional change in transmission at the maximum of the *F* band by an ac method capable of detecting a change in *F*-center concentration of  $10^{11}$  cm<sup>-2</sup>. The crystals used in the study of the dependence of *F*-center production on irradiating wavelength and crystal history were grown both by the Kyropoulos method (seed-pulled) and the Bridgman method (crucible-grown). For seed-pulled KI crystals the *F*-center growth showed a consistent behavior for irradiation throughout the exciton band. The growth was found to be describable as a volume process for which the *F*-center density as a function of the number of photons absorbed per unit volume is given by a saturating curve whose shape and initial slope (quantum efficiency) are approximately independent of irradiating wavelength but whose satura-

tion level increases with decreasing wavelength. The *F*-center saturation density was found to increase from  $5 \times 10^{15}$  cm<sup>-3</sup> for irradiation in the tail of the band to about  $5 \times 10^{17}$  cm<sup>-3</sup> at the peak of the band, with the initial quantum efficiency remaining between 0.1 to 0.2 for this wavelength range. While the behavior for seed-pulled KI samples was relatively unaffected by either plastic deformation or previous irradiation in the exciton band, the crucible-grown samples showed large changes due to either of these treatments. Before these treatments the *F*-center density induced in the crucible-grown samples had predominantly a square-root dependence on the number of absorbed photons; afterwards the behavior was very much like that of the seed-pulled samples. The KBr crystals were found to behave like the seed-pulled KI samples. The results are discussed in terms of the properties of the exciton and its interaction with negative-ion vacancies to form *F* centers.

#### INTRODUCTION

THERE are many questions that remain unanswered as to the physical events that follow the absorption of photons in the fundamental optical bands of an alkali halide crystal. The work of Taft and Phillip<sup>1</sup> has at least tentatively answered the question as to where the dividing line between the region of conducting states (electron-hole pairs) and the region of nonconducting states (excitons) lies in the band. While the existence of nonconducting excited states brought about by excitation in the first fundamental band appears to be reasonably well established, there still remain many questions as to the properties of these excited states. For example, does the energy of excitation remain localized in the lattice or can it move? Also, how in detail does

this excited state bring about the formation of defect centers,<sup>2,3</sup> ionize *F* centers,<sup>4,5</sup> and lead to luminescence at low temperatures?<sup>6</sup>

Smakula's study<sup>2</sup> of the formation of *F* centers in several different alkali halides brought about by excitation in the tail of the first fundamental band (exciton band) indicated that the formation of *F* centers played a most important part in events leading to the destruction of the exciton; i.e., he found approximately unity efficiency for the conversion of photons absorbed in the band to *F* centers formed. The objectives of the present study were to repeat Smakula's experiments and to

<sup>2</sup> A. Smakula, *Z. Physik* **63**, 762 (1930).

<sup>3</sup> N. Inchauspé and G. Chiarotti, *Phys. Rev.* **109**, 345 (1958).

<sup>4</sup> L. Apker and E. Taft, *Phys. Rev.* **79**, 964 (1950); **82**, 814 (1951).

<sup>5</sup> N. Inchauspé, *Phys. Rev.* **106**, 898 (1957).

<sup>6</sup> K. J. Teegarden, *Phys. Rev.* **105**, 1222 (1957).

<sup>1</sup> E. A. Taft and H. R. Phillip, *J. Chem. Phys. Solids* **3**, 1 (1957).

extend the study to excitation as far as possible into the exciton band and thereby to provide further experimental information concerning excitons and their ability to form  $F$  centers.

### EXPERIMENTAL PROCEDURES

The experimental method can be described as follows. A crystal is irradiated with a known number of monochromatic photons, whose wavelength is in the fundamental band, and then the fractional change in transmission at the maximum of the  $F$  band is measured. The fractional change in transmission along with the absorption cross section at the maximum of the  $F$  band yields directly the number of  $F$  centers formed under a unit area. Thus  $F$ -center growth curves can be obtained from a succession of such measurements carried out for increasing irradiation.

#### $F$ -Center Absorption Cross Section

The absorption cross section for  $F$ -centers in KI at 300°K was determined by an optical-chemical method similar to that used by Kleinschrod for KCl,<sup>7</sup> and Doyle for KCl, NaCl, and KBr.<sup>8</sup> The procedure can be described as follows. A large crystal was first additively colored by heating in an atmosphere of potassium vapor. Then the absorption coefficient at the maximum of the  $F$  band (680  $m\mu$ ) was measured for a small sample cleaved from the large crystal and the amount of excess potassium per unit volume was determined for another sample of known volume, also taken from the large colored crystal. The excess potassium of the latter sample was determined by dissolving in water and determining the resultant alkalinity of the solution by a standard colorimetric method. If the assumption is made that to every excess potassium atom in the crystal there corresponds an  $F$  center, the absorption cross section can then be determined from the density of excess potassium and the absorption coefficient at the maximum of the  $F$  band. Two precautions should be observed in making such a determination. First, the

starting crystal should not be too basic or the final alkalinity determination becomes uncertain and second, the colored crystal used in the optical measurement should not contain an appreciable colloidal band in order that the optical measurement be representative of all the excess potassium. The alkalinity of the crystals before being additively colored was never more than 10% of the alkalinity after coloring. The optical measurement was carried out immediately after the colored sample had been quenched from 400°C to 20°C in  $CCl_4$ . There was no sign of a colloidal band for approximately 1–2 hr after the quench. The level to which the crystals were colored varied from 1 to  $5 \times 10^{17}$   $F$  centers/cm<sup>3</sup>. The average value of the absorption cross section obtained from measurements on five different additively colored samples was  $(1.7 \pm 0.2) \times 10^{-16}$  cm<sup>2</sup>. The indicated error is the rms error from these five determinations and the spread is believed to result mainly from the nonuniformity of  $F$ -center density in the large crystals from which the samples for optical and chemical determinations were taken as separate pieces. The value given above may be compared with that obtainable from the data of Rauch and Heer,<sup>9</sup> who effectively measured the cross section by a susceptibility-optical method. The value obtained from their data is  $1.3 \times 10^{-16}$  cm<sup>2</sup>.

The cross section used for KBr was an average of the cross sections obtained from the data of Doyle<sup>6</sup> and Rauch and Heer.<sup>9</sup> This value is  $2.0 \times 10^{-16}$  cm<sup>2</sup>.

#### Irradiation

In order to measure the irradiation intensity, the following procedure was carried out. A standard lamp, calibrated by the National Bureau of Standards, was used to calibrate a thermopile. The thermopile, in turn, was used to calibrate at the three wavelengths 213.9  $m\mu$ , 228.9  $m\mu$ , and 253.7  $m\mu$  (resonance lines of Zn, Cd, and Hg, respectively), an S-11 photomultiplier with uv fluorescing glass (Corning filter No. 3750) mounted in front of the photocathode. The reason for using the uv to visible conversion scheme was that the fluorescent glass plus photomultiplier gave a much more uniform response ( $\pm 1\%$  over an area of 2 cm<sup>2</sup>) over the photocathode than could be obtained with a straight photocell or photomultiplier. The calibrated photomultiplier unit was then used on a day-to-day basis to obtain the irradiating intensity. Since the sensitivity of the photomultiplier unit was found to be approximately constant over the calibration range (a rise of 10% from 253.7  $m\mu$  to 213.9  $m\mu$ ), the same response was assumed to hold to 195  $m\mu$ , the lower limit to the irradiating wavelength used in the study.

The light sources were H-4 mercury arcs for their approximate continuum from 195  $m\mu$  to 235  $m\mu$  and the Cd metal arc for its resonance line at 228.9  $m\mu$ . The passband of the quartz monochromators used with these

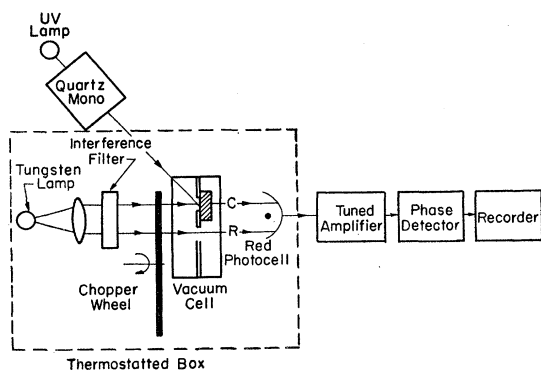


FIG. 1. Schematic diagram of the apparatus.

<sup>7</sup> F. G. Kleinschrod, Ann. Physik **27**, 97 (1936).

<sup>8</sup> W. T. Doyle, Phys. Rev. **111**, 1072 (1958).

<sup>9</sup> C. J. Rauch and C. V. Heer, Phys. Rev. **105**, 914 (1957).

lamps was held at approximately  $2.5 \mu\text{m}$  and with this passband the irradiation flux to the crystal ranged from  $10^{12}$  to  $10^{13}$  photons  $\text{sec}^{-1} \text{cm}^{-2}$ . For wavelengths greater than  $226 \mu\text{m}$  a single quartz monochromator was used, while for wavelengths less than  $226 \mu\text{m}$  a double monochromator was used in order to reduce the effect of scattered light. The area of irradiation was  $0.1 \text{ cm}^2$  and the irradiation times extended from 1 to  $10^5$  sec.

### *F*-Band Transmission Measurement

The fractional change in transmission at the maximum of the *F* band was measured by an ac method. The maximum of the *F* band in KI at  $300^\circ\text{K}$  is at  $680 \text{ m}\mu$  while in KBr it is at  $630 \text{ m}\mu$ . Figure 1 shows the essential features of the apparatus. The crystal was mounted in the vacuum cell. The light for the transmission measurement, which came from a well regulated tungsten lamp, first passed through an interference filter centered at the maximum of the *F* band, and then through a chopper wheel. The filter half-width was about one-tenth of the *F*-band half-width. The chopper wheel allowed the red-sensitive photocell to see alternately, at 7 cps, the reference light beam or the light beam that had passed through the crystal. Figure 2 shows, in a qualitative way, the photocell currents before and after irradiation, where *R* represents the current due to the reference light and  $C_0$  and *C* represent, respectively, the currents due to the light that has passed through the crystal before and after irradiation. Before irradiation the light beams were adjusted such as to make *R* equal to  $C_0$ . Therefore,

$$R = C_0 \propto \text{transmission before irradiation}$$

and

$$C = C_0 e^{-f\sigma} \propto \text{transmission after irradiation,}$$

where *f* is the *F*-center surface density (number of *F* centers formed under unit area) and  $\sigma$  is the absorption cross section at the maximum of the *F* band. Therefore, the fractional change in transmission is

$$(C_0 - C)/C_0 = (R - C)/R = 1 - e^{-f\sigma}.$$

The *F*-center surface density was therefore obtained as the crystal was progressively colored by initially measuring *R* and then following the changes in *R* - *C*.

The growth data were taken by irradiating the crystal in a sequence of periods, such that the number of photons absorbed in each period was increased by a factor of 2 over that in the previous period. In between the successive irradiation intervals, the level to which the *F* band had grown was measured. While there was no intentional bleach between the irradiation intervals, the *F*-light intensity was such that about a 10% reduction in the *F*-center level occurred during the *F*-band transmission measurement. In order to take this bleaching into account in the reduction of the data, the fractional decrease of the *F* band at each transmission measurement was taken as a correction to the photon number up to that measurement.

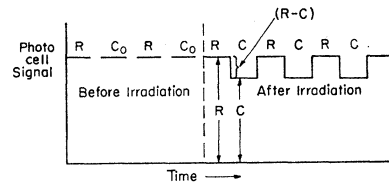


FIG. 2. Photocell current before and after irradiation. *R* is the photocell current due to the reference light beam and  $C_0$  and *C* are respectively the currents due to the light beam that passes through the crystal before and after irradiation.

The lower limit to the fractional change in transmission that could be measured (unity signal to noise) was found to be set by several different factors and in practice was approximately  $1:10^5$ . This limit corresponded to a change in *F*-center surface density of approximately  $10^{11} \text{ cm}^{-2}$ . The main source of long-term drift was found to be due to changes in room temperature which resulted in slow changes in *R*-*C* due to the thermal expansion and contraction of the optical apparatus. This long term drift was reduced to  $1:10^5$  by enclosing the entire optical apparatus in a thermostated enclosure (indicated by dotted box in Fig. 1) regulated to  $\pm 0.2^\circ\text{C}$ . The short-term noise was set by the shot noise in the photocell current. By providing sufficient *F*-light intensity, the effect of this noise was also reduced to  $1:10^5$ .

### Crystals

The crystals used in the present study were grown by the Bridgman method (crucible-grown) at Harshaw Chemical Company and grown by both the Kyropoulos method (seed-pulled) and the Bridgman method at the Westinghouse Research Laboratory. The crystals grown at this Laboratory were grown from melts of Reagent grade salt in platinum crucibles in an argon atmosphere. Both spectroscopic and ionic conductivity measurements have indicated that these crystals are of comparable purity to those obtained from the Harshaw Chemical Company. The samples that were to be thicker than 0.1 cm were cleaved to size. The samples thinner than 0.1 cm were first ground and then chemically polished in order to remove the damage due to grinding. The chemical polish consisted of successive rinses in ethyl alcohol, isopropyl alcohol, and carbon tetrachloride. The ethyl alcohol served to remove the bulk of the damaged surface (rate of removal  $\approx 0.003 \text{ cm/min}$  for KI) and the other two acted as rinses. The plastic deformation was carried out by simple compression in a small machinist's vise.

## RESULTS

### Effect of Water Vapor on *F*-Center Growth

At the initiation of the present study the KI crystals under study were simply mounted in an optical cell containing room air. It was found that for irradiation wavelengths shorter than approximately  $230 \text{ m}\mu$ , there

was no detectable growth in the  $F$  band. However, if the cell was evacuated, the growth of  $F$  centers could be obtained for irradiation anywhere in the fundamental band. The effect was found to be reversible in that after exposure to room air (decrease in colorability for irradiation at the peak of the first fundamental band took approximately 10 min) the cell could be pumped out and the colorability was returned to its initial value. Water vapor was suspected as the cause of the effect so the following tests were made. Water was frozen in the vacuum system at liquid  $N_2$  temperature and then the system was exhausted. At the peak of the first fundamental band the usual colorability was obtained. The temperature of the ice was raised to  $-20^\circ\text{C}$  (ice, water, and  $\text{NaCl}$ ) and the ability to color was lost in 3 to 5 min. Again the ice temperature was reduced to the liquid  $N_2$  point and the colorability returned. To be sure that only  $\text{H}_2\text{O}$  affected the colorability and not the permanent gases, the system was filled from Linde flasks of  $\text{O}_2$  or  $\text{N}_2$ . These gases were found to have no effect for times of the order of hours. It was therefore concluded that water vapor did decrease the colorability while the permanent gases did not. The data that follows were obtained with samples mounted in an evacuated cell (pressures  $\approx 10^{-5}$  mm Hg).

### KI, Seed-Pulled

The desirability of studying  $F$ -center growth under conditions of spatially uniform irradiation is obvious. However, in order to have uniform irradiation it is necessary that the sample be thin in comparison to the reciprocal of the absorption coefficient. Figure 3 gives the absorption coefficient ( $\alpha$ ) for the wavelength range pertinent to the present study for KI and KBr as given

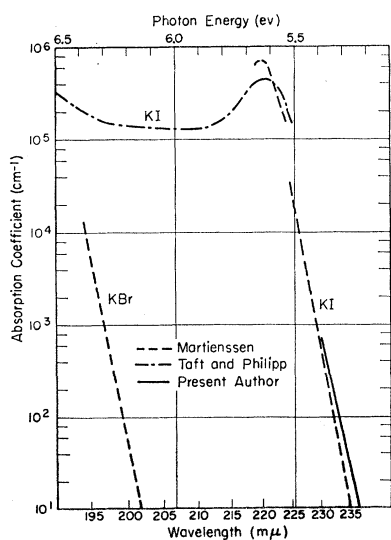


FIG. 3. Absorption coefficient versus wavelength in the first fundamental band (exciton band) for KI and KBr at  $300^\circ\text{K}$ .

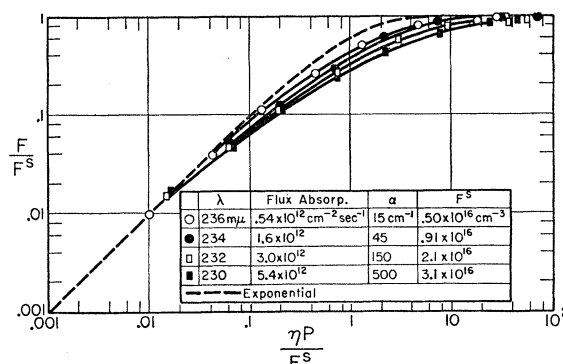


FIG. 4. Ratio of  $F$ -center volume density ( $F$ ) to  $F$ -center volume saturation density ( $F^0$ ) versus the product of the initial quantum efficiency ( $\eta$ ) and number of photons absorbed per unit volume ( $P$ ) divided by the  $F$ -center saturation volume density ( $F^0$ ) for a 0.0064 thick KI sample under conditions of uniform volume irradiation.  $\eta = 0.2$  for all wavelengths. The flux absorbed as given in the table represents the number of photons absorbed per unit area per unit time.

by Martienssen,<sup>10,11</sup> Taft and Phillip,<sup>1</sup> and as obtained by the present author. From Fig. 3 it is clear that because of the extremely large values of  $\alpha$  near and beyond the peak of the exciton band it is not practical to satisfy the condition for uniform irradiation with single crystal samples for the entire wavelength range. Therefore, in the present study, measurements were carried out with uniform irradiation as far as possible into the exciton band by using the thinnest available samples. The results of these measurements were then used as a guide for interpreting the results under conditions of non-uniform irradiation with samples that were thick in comparison to  $1/\alpha$ .

### Thin Samples

$F$ -center growth data were obtained for conditions of uniform irradiation by using samples whose thickness was of the same order or less than the reciprocal of the absorption coefficient ( $\alpha$ ) corresponding to the irradiating wavelength used. With samples ranging in thickness from 0.0064 cm to 0.11 cm, it was possible to make measurements for a range of  $\alpha$  from  $15 \text{ cm}^{-1}$  to  $500^{-1}$  which corresponded to the wavelength range of 236 to 230  $m\mu$ .  $F$ -center growth for seed-pulled samples was found to be essentially unaffected by previous irradiation; i.e., a crystal could be filled with  $F$  centers and bleached out any number of times and the subsequent growth behavior remained essentially the same as that for the freshly prepared sample. This meant, that for a given sample thickness, growth runs for different irradiating wavelengths could be carried out on the same sample. Figure 4 shows the growth curves that were obtained with a 0.0064-cm-thick sample. It was found that the similarity between the data obtained at different irradiating wavelengths could be most clearly dis-

<sup>10</sup> W. Martienssen, J. Phys. Chem. Solids **8**, 294 (1959).

<sup>11</sup> W. Martienssen, J. Phys. Chem. Solids **2**, 257 (1957).

played by plotting the results in the normalized manner of Fig. 4. The initial quantum efficiency ( $\eta$ ) as used in plotting the results was taken as the ratio of *F* centers formed to photons absorbed at the lowest measured *F*-center level. The value of this quantity was very close to 0.2 for all the curves in Fig. 4. For seed-pulled samples at irradiation wavelengths greater than 230  $m\mu$  the *F*-center growth at the lowest measurable *F*-center level was found to be very close to being linear with absorbed photons. This is illustrated by the initial part of the curves in Fig. 4. Therefore, in this case the initial quantum efficiency, as defined above, coincides with the more conventional usage of the term, i.e., equal to the slope of the linear region. While the initial quantum efficiency was found to be independent of wavelength, the *F*-center saturation density ( $F^s$ ) was found to increase with decreasing wavelength. The values for  $F^s$  corresponding to the different curves in Fig. 4 are given in the table of that figure.

For purposes of comparison the exponential curve

$$F/F^s = 1 - \exp(-\eta P/F^s),$$

is plotted along with the experimental data in Fig. 4, where  $F$  is the *F*-center volume density,  $P$  is the number of photons absorbed per unit volume, and  $\eta$  and  $F^s$  are defined above. It is to be noted that the experimental curves group reasonably close together and do not deviate far from an exponential. The small deviation that does exist grows larger as the wavelength becomes shorter. These normalized curves are representative of the data obtained for other thin samples of thickness equal to or greater than 0.0064 cm. Of course, as the sample becomes thicker, the maximum absorption coefficient at which the measurements may be made with uniform irradiation becomes smaller.

The *F*-center saturation density as a function of wavelength is shown in Fig. 5 for samples of various

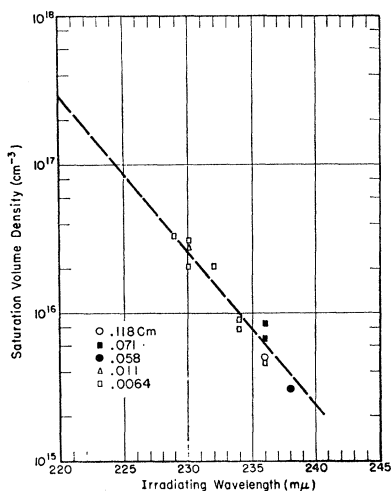


FIG. 5. *F*-center saturation volume density versus irradiating wavelength for KI sample of various thicknesses under conditions of uniform volume irradiation.

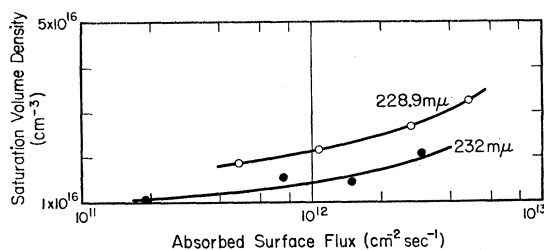


FIG. 6. *F*-center saturation volume density versus absorbed surface flux (number of photons absorbed per unit area per unit time) for a 0.0064-cm thick KI sample under conditions of uniform volume irradiation.

thicknesses. The rate at which photons were absorbed per unit volume was not the same at the different wavelengths in Figs. 4 and 5 but increased with decreasing wavelength. The question therefore arises as to whether the increase in saturation density is related to the decrease in wavelength or to the increase in photon absorption rate. A typical value for the increase of photon absorption rate in going from 236 to 230  $m\mu$  can be obtained from the increase in absorbed surface flux given in the table of Fig. 4. The factor can be seen to be about 10 for this wavelength range. Figure 6 shows data obtained with the 0.0064-cm sample for the dependence of the saturation density on absorbed surface flux (proportional to volume photon absorption rate) for the two wavelengths 228.9 and 232  $m\mu$ . It is evident from Fig. 6 that an increase in photon absorption rate by a factor of 10 results in not more than a 50% increase in saturation density. From Figs. 4 and 5, when the wavelength is decreased from 236 to 230  $m\mu$  with the photon rate increased by a factor of 10, the saturation density is increased by a factor of 6. Therefore, it must be concluded that the increase in the *F*-center saturation density is related to the decrease in irradiation wavelength and not to the increase in photon absorption rate.

Another question that can be asked is whether the *F*-center production is truly a volume process. Figure 7 shows how the saturation surface density (maximum number of *F* centers formed under unit area) depends on sample thickness for irradiation at 236  $m\mu$ . It is evident that the data lies reasonable close to a straight line that passes through the origin. This is the behavior one would expect for a volume process. This same dependence has also been obtained at shorter wavelengths.

### Thick Samples

*F*-center growth studies could not be carried out with uniform irradiation at wavelengths such that  $\alpha > 500$   $cm^{-1}$  because thin enough samples were not available. Therefore, the samples were necessarily thick in comparison to  $1/\alpha$  in this wavelength region. With thick samples, growth studies were made over a wavelength range of 236 to 200  $m\mu$ , which meant that these measurements overlapped the thin sample work in the region where  $\alpha < 500$   $cm^{-1}$ . Figure 8 shows typical growth

curves for wavelengths extending from 236 to 220 m $\mu$ . It is evident from Fig. 3 that this range extends from the tail (15 cm<sup>-1</sup>) up to the peak of the exciton band. For wavelengths from 220 to 200 m $\mu$ , the growth curves were found to differ only slightly from the 220-m $\mu$  curve (10–20% higher at high photon levels) and are not shown in Fig. 8. It is to be noted that the curves order themselves according to the irradiation wavelength with the highest curve corresponding to the longest wavelength. Also, the initial quantum efficiency lies in the range of 0.1 to 0.2 over the entire wavelength range. Here, as above, the initial quantum efficiency is the ratio of  $F$  centers formed to photons absorbed at the lowest measured  $F$ -center concentration.

The question now arises as to whether the results obtained with thick samples are consistent with those found for thin samples with uniform irradiation. With thin samples it was found that the  $F$ -center growth behavior could be described by a saturating function similar to a charging exponential. Let this functional dependence be given by

$$F/F^s = S(\eta P/F^s),$$

where  $S$  is a saturating function. The  $F$ -center surface density for a sample that is thick in comparison to  $1/\alpha$  will then be given by the integral

$$f = \int_0^\infty F dz = F^s \int_0^\infty S[\eta P(z)/F^s] dz,$$

where  $f$  is the  $F$ -center surface density,  $z$  is the distance into the sample, and  $P(z)$  is the number of photons absorbed per unit volume at  $z$ . This expression implies that any effects due to the surface or due to the spreading (diffusion) of the process over distances comparable to  $1/\alpha$  are neglected. Now  $P(z)$  will be given by  $\rho\alpha e^{-\alpha z}$ , where  $\alpha$  is of course the absorption coefficient corre-

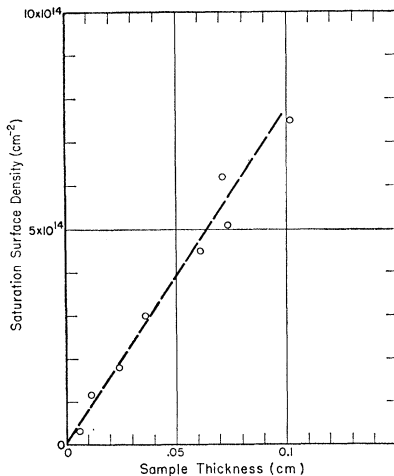


FIG. 7.  $F$ -center saturation surface density versus sample thickness for the irradiation wavelength of 236 m $\mu$ , under conditions of uniform volume irradiation for KI samples.

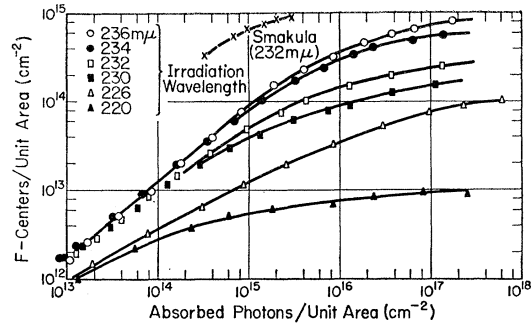


FIG. 8. Number of  $F$ -center formed per unit area versus number of photons absorbed per unit area for seed-pulled KI samples whose thickness was large in comparison to  $1/\alpha$ . The uppermost curve gives the data obtained by Smakula for irradiation at 232 m $\mu$ .

sponding to the irradiating wavelength and  $\rho$  is the number of photons absorbed per unit area. Therefore

$$f = F^s \int_0^\infty S(\rho\eta\alpha e^{-\alpha z}/F^s) dz.$$

If we let  $\rho\eta\alpha e^{-\alpha z}/F^s = U$ , then

$$f = (F^s/\alpha) \int_0^{\rho\eta\alpha/F^s} S(U) dU/U.$$

Now it is clear that when  $U$  is large,  $S(U) \rightarrow 1$  and therefore

$$f = \text{const} + F^s/\alpha \ln \rho,$$

and

$$df/d \ln \rho = F^s/\alpha.$$

Therefore, if the growth behavior for thick samples is consistent with the behavior found for thin samples, we would expect the following to hold: (1)  $f\alpha/F^s$  will be approximately the same function of  $\rho\eta\alpha/F^s$  for all wavelengths, and (2) at large  $\rho$ ,  $f$  will vary as the  $\ln \rho$  and the slope of the logarithmic dependence will be equal to  $F^s/\alpha$ .

When the results for thick samples were plotted in a semilog manner, the curves were found to be linear at high photon level. Figure 9 gives the results for  $F^s$  obtained from the slope of the logarithmic dependence from the data in Fig. 8 as well as from data for other thick samples. The solid line in Fig. 9 represents the average behavior for thin samples. It is seen that the results from thick and thin samples are reasonably consistent with each other over the wavelength range covered by both, and that the high absorption coefficient data from thick samples also agree reasonably well with the extrapolation of the thin-sample curve to shorter wavelengths. It should also be possible to plot the thick-sample data in a normalized way as is indicated by expression for the surface density ( $f$ ) as developed above. Figure 10 shows such a replot of the data given in Fig. 8 along with a curve representing the behavior

for a thick sample if the unit volume behavior were exponential. It is evident, as was found for thin samples, that the data do not deviate far from an exponential behavior with the possible exception of the 226- $\mu$ m data.

The results presented above have been for crystals grown from melts of Reagent-grade salt. It is natural to ask what effect greater impurity concentration would have on the *F*-center growth behavior. KI crystals were grown (seed-pulled) from melts containing respectively 0.1% by weight of  $\text{CaI}_2$ ,  $\text{K}_2\text{S}$ , and  $\text{K}_2\text{NO}_3$ . Measurements of the *F*-center growth in these samples have shown them to behave in most respects like the samples grown from Reagent-grade salt. That is, both the initial quantum efficiency and the shape of the growth curves (thick samples) were unchanged. However, the *F*-center saturation density appeared to be somewhat enhanced by added impurities, e.g., for the  $\text{CaI}_2$ -doped sample the saturation density for irradiation at 235  $\mu$ m was about twice the value given in Fig. 9 at this same wavelength.

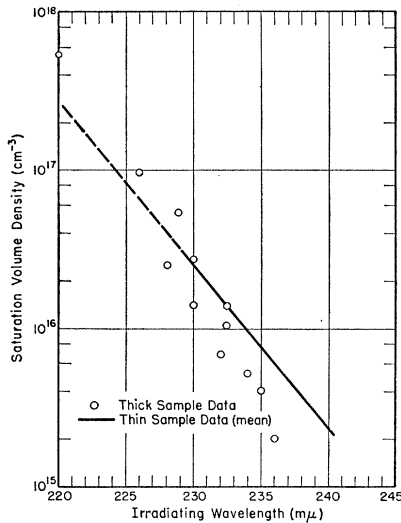


FIG. 9. *F*-center saturation volume density versus irradiating wavelength for seed-pulled KI samples whose thickness was large in comparison to  $1/\alpha$ .

### KI, Crucible-Grown

Figure 11 gives the growth data obtained with Harshaw crucible-grown samples for irradiating wavelengths completely spanning the exciton band. The samples that were used to obtain the growth curves were thick in comparison to the penetration depth of the irradiating light and had not been previously irradiated. Here, as was also found for seed-pulled samples, for irradiation wavelengths beyond the peak of the exciton band (less than 220  $\mu$ m) the growth curves lie very close together. These curves show a very similar behavior to those of the seed-pulled samples. However, for longer wavelengths the curves differ appreciably from those for seed-pulled samples, in that they do not rise as high at a given irradiation level nor do they have the same

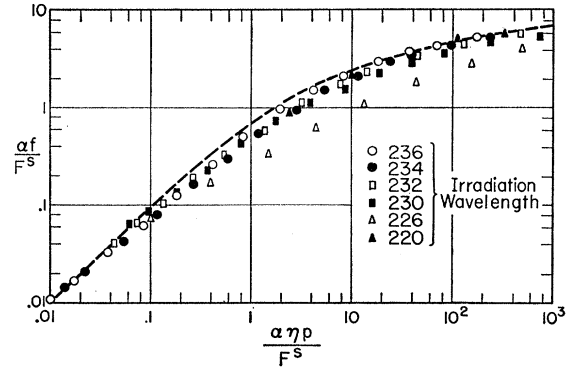


FIG. 10. Normalized replot of the data given in Fig. 8; the product of absorption coefficient ( $\alpha$ ), *F*-center surface density ( $f$ ), and the reciprocal of *F*-center saturation volume density ( $F^0$ ) versus the product of the absorption coefficient ( $\alpha$ ), the initial quantum efficiency ( $\eta$ ), the number of photons absorbed per unit area ( $\rho$ ), and the reciprocal of the *F*-center volume saturation density ( $F^0$ ).

shape. It is seen at these longer wavelengths that over many decades of irradiation the curves are remarkably close to a square-root dependence. The crucible-grown samples from this laboratory have shown this same general behavior.

While with the seed-pulled samples it was found that neither previous irradiation nor plastic deformation appreciably affected the *F*-center growth behavior, with crucible-grown samples these two treatments were found to effect large changes. In fact, while the crucible-grown samples behaved quite differently from seed-pulled samples before either of these treatments, afterwards the crucible-grown behavior was very much like that found for the seed-pulled. Figure 12 shows the growth data for a Harshaw sample before and after a deformation of 5.5% for the irradiation wavelengths of 228.9  $\mu$ m. These data were taken with two different samples without previous irradiation. Also plotted, for comparison, are data obtained with a seed-pulled sample. Figure 13 illustrates the effect of previous irradiation on the growth behavior of a Harshaw crucible-grown sample. Here the various curves represent successive

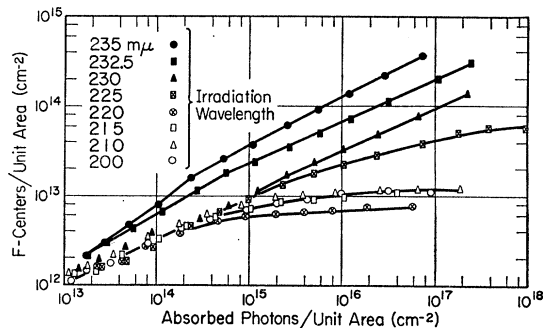


FIG. 11. Number of *F* centers formed per unit area versus number of photons absorbed per unit area for crucible-grown (Harshaw) KI samples whose thickness was large in comparison to  $1/\alpha$ .

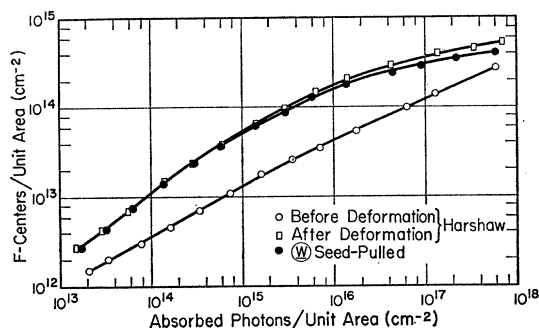


FIG. 12.  $F$ -center growth curves showing the effect of plastic deformation on the behavior of crucible-grown (Harshaw) KI sample at irradiation wavelength of  $228.9 \mu\mu$ . The sample thickness was large in comparison to  $1/\alpha$ .

irradiation runs on the same sample to successively higher  $F$ -center densities. After each run, the  $F$  centers were completely bleached with white light. It is evident that irradiation produces definite changes in the subsequent growth and tends to change the behavior to that found for seed-pulled samples. Another feature to note is that each of the curves after having passed the maximum  $F$ -center level of the just previous curve appears to join onto an extrapolation of the first curve.

### KBr

The measurements that were made on KBr crystals only extended part way into the exciton band because of the difficulties of obtaining sufficient irradiation intensity at the shorter wavelengths. Figure 14 shows the results for Harshaw samples for the wavelengths 200 and  $195 \mu\mu$ . It will be noted that the curves are very similar in shape and initial effective quantum efficiency (0.2) to those obtained with seed-pulled KI. These data, when plotted in a semilog manner, yielded a straight line portion at high irradiation level, the slope of which gives, as was carried out for seed-pulled KI data, the  $F$ -center saturation density ( $F^s$ ). The values obtained for  $F^s$  are given in the table of Fig. 14. It is worth noting that the two saturation values for KBr are close to the values obtained for seed-pulled KI at the corresponding values of absorption coefficient. Measurements carried out on seed-pulled KBr samples grown in this laboratory yielded very similar results to those obtained with Harshaw samples and neither of these two types of samples showed appreciable effects due to previous irradiation. No thin-sample measurements were made for KBr.

### DISCUSSION

The physical ideas that must necessarily enter into the discussion of the results and for which clarification is desirable are concerned both with the properties of the exciton and of the negative-ion vacancies which when filled with electrons form the observed  $F$  centers. A simple model for the coloration process which can serve

as a starting point for discussion can be described as follows; an exciton, which is formed in a crystal containing some initial concentration of negative-ion vacancies, travels to a vacancy and there gives up its electron to form an  $F$  center. The hole that is left behind drifts off and is trapped elsewhere in the crystal. When this picture is translated into rate equations for vacancies and  $F$  centers and the assumption is made that the exciton has a lifetime independent of vacancy and  $F$ -center concentration, the volume growth expression that results is an exponential given by

$$F/V_0 = 1 - \exp(-\tau\beta P).$$

In this expression  $V_0$  is the initial vacancy concentration,  $\tau$  is the exciton lifetime and  $\beta$  is the coefficient which, when multiplied by the product of the vacancy and exciton concentration, gives the rate of vacancy decay or  $F$ -center buildup. The derivation of this expression is given in the Appendix.

The shape of the growth curves and the initial quantum efficiency obtained for seed-pulled KI crystals and for all types of KBr crystals are at least reasonably consistent with this model; i.e., the shape was shown to be close to an exponential and the value of 0.2 for the initial quantum efficiency would indicate that the part played by vacancies in limiting the exciton lifetime is reasonably small. The fact that the initial quantum efficiency is approximately independent of irradiating wavelength would imply that the parameters that characterize the process of an exciton filling a vacancy are independent of where in the exciton band the photon is absorbed. While these two aspects of the data seem to be consistent with the simple model, the result that the saturation density increases with decreasing wavelength is not. The model would predict a saturation density independent of wavelength because of the assumed definite vacancy density. The above remarks would suggest that while the idea of filling free vacancies to form  $F$  centers seems to be reasonable at the start of the  $F$ -center growth, near saturation the picture must be extended to account for the increasing saturation density. The increase in saturation density implies that the shorter wavelength excitons have the ability to introduce vacancies that were not initially available for direct filling. This difference in the behavior of the excitons formed by excitation at different points in the exciton band also implies that the excitons retain some memory of where in the exciton energy band they originated. This in turn might suggest that they are not completely thermalized in their lifetime, with the difference in behavior being due to the difference in their initial energy. Also the increased deviation from an exponential behavior which is correlated with the increasing saturation density may be related to the suggested change in mechanism near saturation.

The  $F$ -center growth behavior for seed-pulled samples was found to be unaffected by previous irradiation; i.e.,

the  $F$ -center saturation density that is obtained for a certain sample at some particular wavelength is not affected as a result of the sample having been previously filled with  $F$  centers to a higher density. This behavior must mean that even though a high vacancy concentration exists in a sample that has been irradiated to a high  $F$ -center density, after the  $F$  centers are destroyed (bleached) the vacancy concentration does not remain at a level equal to the  $F$ -center concentration before bleach, but decays very quickly to some lower concentration. More direct evidence for this type of vacancy decay in KI crystal has been obtained by Delbecq *et al.*<sup>12</sup> in their studies of the  $\alpha$  band. The possibility that the vacancy concentration may return to some lower fixed level may explain why the value found for the initial quantum efficiency is independent of the saturation density (or irradiation wavelength); i.e., a definite vacancy concentration exists at the initiation of coloring.

The results for crucible-grown KI samples, whether Harshaw or grown in this laboratory, which demonstrate that previous irradiation changes the growth behavior and tends to make the behavior approach that of seed-pulled samples would suggest that the crucible-grown samples have a very small initial concentration of free vacancies and that the  $F$ -center growth involves the introduction of new vacancies. If, after such an initial growth, the  $F$  centers are destroyed by bleaching there would remain a higher concentration of free vacancies than were present initially which could then be filled in the manner suggested for the seed-pulled samples. The vacancies that are brought in as a result of irradiation might be initially in the form of vacancy clusters or tied to impurities and in this form would be unavailable for direct filling. However, the decay of an exciton at the cluster or impurity could result in the release of a vacancy that could then be directly filled. It is not unreasonable to expect that plastic deformation

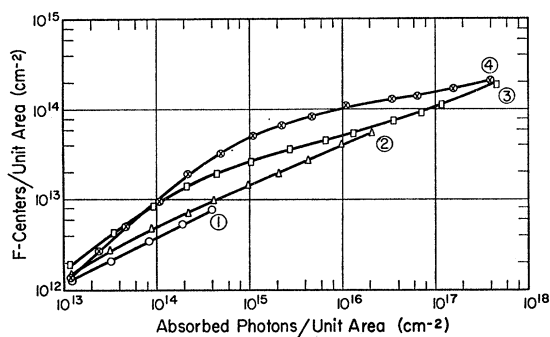


FIG. 13.  $F$ -center growth curves for a crucible-grown (Harshaw) KI sample showing the effect of previous irradiation at irradiation wavelength of 228.9  $m\mu$ . The numbered curves represent successive irradiation runs taken to increasingly higher  $F$ -center levels, with the  $F$  centers removed (bleached) between each run. Curve 1 represents the first run on the "as grown" sample. The sample thickness was large in comparison to  $1/\alpha$ .

<sup>12</sup> C. J. Delbecq, P. Pringsheim, and P. Yuster, *J. Chem. Phys.* **19**, 574 (1951).

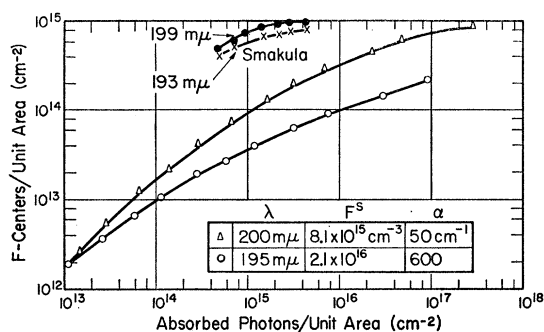


FIG. 14.  $F$ -center growth curves for Harshaw KBr samples whose thickness is large in comparison to  $1/\alpha$ ; the irradiation wavelengths were 200 and 195  $m\mu$ . The two uppermost curves represent the results obtained by Smakula for irradiation at 193 and 199  $m\mu$ .

could also cause the release of vacancies from these sources and would explain the effect that plastic deformation had on crucible-grown samples. The fact that crucible-grown samples seem to have much fewer initial vacancies than the seed-pulled samples is not unexpected, for the crucible-grown samples are grown at a rate ten times slower than the seed-pulled samples. This should give the vacancies a better opportunity to relax to a lower concentration.

On general grounds it is to be expected that the exciton-induced  $F$ -center process plays some part in the x-ray and  $\gamma$ -ray coloration mechanism. The  $F$ -center growth curves that are obtained with either of these high-energy irradiations have been shown to be made up of an exponential fast growth followed by a linear slow growth.<sup>13,14</sup> The fast growth is believed to represent the filling of existing vacancies while the slow growth represents the production and filling of new vacancies.<sup>13,14</sup> The fast growth carries the  $F$ -center density up to  $10^{16}$  to  $10^{17}/\text{cm}^3$  and the slow growth follows, carrying the density to a saturation of  $10^{18}$  to  $10^{19}/\text{cm}^3$ . The fact that the exciton-induced  $F$ -center growth is very similar, both in growth curve shape and in saturation density, to the fast-growth region of  $\gamma$  or x-ray coloration indicates that excitons may be important in this region. However, without information as to the relative number of electrons and excitons that are produced by these high-energy photons, it is not possible to give a quantitative estimate of the importance of the excitons. The fact that the present studies have shown that excitons cannot produce  $F$ -center densities higher than  $\approx 10^{17}/\text{cm}^3$  seems to suggest that excitons are not important in the slow-growth region. This should be contrasted with the recent suggestion by Smoluchowski *et al.*<sup>14</sup> that it is the excitons that produce the new vacancies in the slow-growth region.

The data, as shown in Fig. 11 for crucible-grown KI crystals, show a remarkably large regime, both in irradiating wavelength and photon level, over which the

<sup>13</sup> R. B. Gordon and A. S. Nowick, *Phys. Rev.* **101**, 977 (1956).

<sup>14</sup> P. V. Mitchell, D. A. Wiegand, and R. Smoluchowski, *Phys. Rev.* **121**, 484 (1961).

$F$ -center density has a square-root dependence on the number of absorbed photons. This type of dependence implies that the rate (quantum efficiency) of  $F$ -center growth is inversely proportional to the  $F$ -center density. It was suggested above that this type of crystal contains a very small initial vacancy concentration and that the square-root-dependent growth that characterizes these crystals is related to introduction and filling of vacancies that were initially unavailable for direct filling. It might be expected that in the case of vacancies being introduced and immediately filled, there would be a quasi-balance between these two rates that would result in a reasonably constant vacancy concentration. With the rate of  $F$ -center growth being proportional to the product of vacancy and exciton concentration, the experimental result that the growth rate is inversely proportional to the  $F$ -center density would imply that the exciton density or exciton lifetime has this same dependence. This seems to indicate, at least when the vacancy concentration is small, that  $F$  centers act as a dominant destruction center for excitons. This lifetime limitation may be related to the results of studies by Apker *et al.*<sup>4</sup> and Inchaupé<sup>5</sup> which indicated that excitons have a finite probability of ionizing  $F$  centers.

The result that the initial quantum efficiency was always found in the range of 0.1 to 0.2 is in disagreement with the value of unity found by Smakula.<sup>2</sup> The results obtained by Smakula are plotted in Figs. 8 and 14. The values obtained in the present study for the number of irradiating photons and for the change in  $F$ -center concentration are not in error by more than 20 to 30%. It is possible that the crystals studied by Smakula contained many more initial vacancies than those of the present study, such an increased vacancy density, on the basis of the simple filling model, would lead to a higher quantum efficiency. However, every effort in the present study to increase the vacancy concentration by added impurities or plastic deformation did not seem to affect appreciably the initial quantum efficiency.

It is reasonable to suggest that a representative value for the diffusion distance of an exciton is given by the average distance between the vacancies initially present in a crystal. An order of magnitude value for the initial vacancy concentration in the seed-pulled samples can be taken as the smallest value given for the  $F$ -center

saturation density in Figs. 5 and 9. The value for the vacancy concentration is  $\approx 10^{15}/\text{cm}^3$  and therefore the exciton diffusion distance is  $\approx 10^{-5}$  cm. The fact that the depth to which excitons are formed ( $1/\alpha$ ) only reaches this value for irradiation near the peak of the exciton band may explain why the results are consistent with a volume process with the effects due to the surface or to diffusion over distances greater than  $1/\alpha$  being unimportant.

A few remarks should be made concerning the effect that water vapor was found to have an  $F$ -center growth. It is reasonable to suggest that water molecules can diffuse into the sample and act as destruction centers for excitons. The fact that the effect becomes larger, the smaller the penetration depth of the irradiating light is consistent with this view. However, since no detailed study was made of this effect, it is not possible to draw more definite conclusions.

#### APPENDIX

If the exciton has a lifetime  $\tau$ , the exciton concentration ( $X$ ) will be given by

$$X = \tau dP/dt, \quad (1)$$

where  $dP/dt$  is the rate at which photons are absorbed per unit volume. Now the rate of vacancy decay and  $F$ -center buildup is given by

$$-dF/dt = dV/dt = -\beta VX, \quad (2)$$

where  $V$  is the vacancy concentration,  $F$  is the  $F$ -center concentration, and  $\beta$  is a parameter characterizing the exciton-vacancy interaction. When the expression for the exciton concentration (1) is inserted in (2), one obtains

$$-dF/dP = dV/dP = -\beta\tau V. \quad (3)$$

The integration of Eq. (3) results in

$$V = V_0 e^{-\beta\tau P}, \quad (4)$$

and

$$V = V_0 - F, \quad (5)$$

where  $V_0$  is the initial vacancy concentration. Equations (4) and (5) can then be combined to yield

$$F/V_0 = 1 - \exp(-\beta\tau P).$$